

## On the Development of a Model for the Prediction of Liquid Loading in Gas Wells with an Inclined Section

Mengna Liao<sup>1,2</sup>, Ruiquan Liao<sup>1,2</sup>, Jie Liu<sup>1,2,\*</sup>, Shuangquan Liu<sup>3</sup>, Li Li<sup>3</sup>, Xiuwu Wang<sup>1,2</sup> and Yang Cheng<sup>1,2</sup>

**Abstract:** The ability to predict liquid loading in horizontal gas wells is of great importance for determining the time of drainage and optimizing the related production technology. In the present work, we describe the outcomes of experiments conducted using air-water mixtures in a horizontal well. The results show that the configuration with an inclined section is the most susceptible to liquid loading. Laboratory experiments in an inclined pipe were also conducted to analyze the variation of the critical gas flow rate under different angles, pressure and liquid volume (taking the equal liquid volume at inlet and outlet as the criterion for judging on the critical state). According to these results, the related angle of the inclined section ranges from 45° to 60°. Finally, a modified approach based on the Belfroid model has been used to predict the critical gas flow rate for the inclined section. After comparison with field data, this modified model shows an accuracy of 96%, indicating that it has better performances with respect to other models used in the past to predict liquid loading.

**Keywords:** Horizontal gas well, inclined section, liquid loading, critical gas flow rate, air-water flow.

### 1 Introduction

During the development of gas reservoir, liquid loading is usually one of the most serious production problems. In the early stages of production, high gas flow rate is capable of carrying the produced liquid to the surface. With the reservoir energy gradually depleting, the rapid reduction of gas flow rate results in liquid accumulation at the bottom of the wellbore. As a consequence of liquid loading, an increase in the back pressure in the well causes the available transport energy to decrease until eventually liquid accumulates completely ceasing production. Therefore, an accurate prediction of critical liquid carrying gas flow rate is of great significance for extending the production life of the gas

---

<sup>1</sup> School of Petroleum Engineering, Yangtze University, Wuhan, 430100, China.

<sup>2</sup> Laboratory of Multiphase Pipe Flow of Gas Lift Innovation Center, CNPC (Yangtze University), Wuhan, 430100, China.

<sup>3</sup> Oil and Gas Technology Research Institute of Changqing Oilfield Company, Xi'an, 710000, China.

\* Corresponding Author: Jie Liu. Email: fatestrenlj@yahoo.com.cn.

well [Liu, Luo, Zhang et al. (2018); Yang, Wang, Chen et al. (2009); Chen, Yao, Han et al. (2016); Li, Li, Teng et al. (2014); Xiao, Li and Yu (2010)].

Many researchers have done a lot of work to predict the onset of liquid loading, but its mechanism still remains controversial. Turner et al. [Turner, Hubbard and Dukler (1969)] initially proposed a liquid-film model and an entrained-droplet model, and eventually adopted the spherical droplet model to predict the critical gas velocity for vertical wells. Coleman et al. [Coleman, Clay, McCurdy et al. (1991)] suggested that the critical flow rate, required to keep low-pressure gas wells (wellhead pressure less than 3.45 MPa) unloaded can be predicted adequately with the Turner et al. (1969) model without the 20% upward adjustment. Later, Nossier et al. [Nosseir, Darwich, Sayyoub et al. (2000); Li, Li and Sun (2001); Guo, Ghalambor and Xu (2006); Wang and Liu (2007); Zhou and Yuan (2010); Wang, Bai, Zhu et al. (2015)] have put forward modified models on the basis of Turner et al. (1969) droplet model. Meanwhile, other researchers Barnea et al. [Barnea (1986); van 't Westende, Kemp, Belt et al. (2007); Belfroid, Schiferli, Alberts et al. (2008); Veecken, Hu and Schiferli (2010) propose that liquid loading is controlled by the film reversal.

Currently, only a few studies have been conducted that deal with liquid loading for horizontal gas wells. Luo et al. [Luo, Kelkar, Pereyra et al. (2014)] developed a comprehensive model that is based on the Barnea (1986) model. The new model took into account the non-uniform film thickness of the pipe and thus it improved the prediction of liquid loading in deviated wells. Shi et al. [Shi, Sun and Li (2016)] proposed a half-hamburger droplet model to calculate the critical liquid loading flow rate for multi-fractured horizontal gas wells based on experiments in a gas flow wellbore with different inclined angles. Shekhar et al. [Shekhar, Kelkar, Hearn et al. (2017)] assumed that liquid loading initiates when the liquid film starts falling backward and proposed a new method to predict the onset of liquid loading for inclination angles. Wang et al. [Wang, Guo, Zhu et al. (2018)] developed a film model from force balance of the bottom film of the inclined tubing accounting for bottom-film thickness and gas/liquid interfacial friction factor to reveal the liquid loading mechanism.

Most studies on liquid loading were conducted for vertical wells. The calculation models for the critical flow rate of gas-liquid two-phase flow in horizontal wells were also based on vertical wells [Wang and Li (2012); Alsaadi, Pereyra and Torres (2015); Li, Zhang, Yang et al. (2012); Jiang, Zou, Zhou et al. (2012); Zhang, Luo, Liu et al. (2019)]. In fact, the study of liquid loading for horizontal wells is more complicated than that of vertical wells, considering the effects of flow pattern transition and inclination [Wang, Li, Wang et al. (2014)]. With the increasing number of horizontal wells, it is urgent to study the liquid loading in horizontal gas wells. In this paper, experimental investigation has been systematically conducted to determine the position of the easiest to liquid loading and to analyze the effect of inclined angle, pressure and liquid volume flow rate on the critical gas flow rate of horizontal gas wells. The experimental phenomenon and test data are used to analyze the variation law of critical gas velocity. We optimized the Belfroid et al. (2008) model by modifying its angle-correction term, ultimately developed a modified mathematical model for predicting critical gas flow rate of inclined section in horizontal gas wells, providing an experimental basis for the understanding of liquid loading.

## **2 The easiest to liquid loading section in horizontal gas wells**

### **2.1 Theoretical basis**

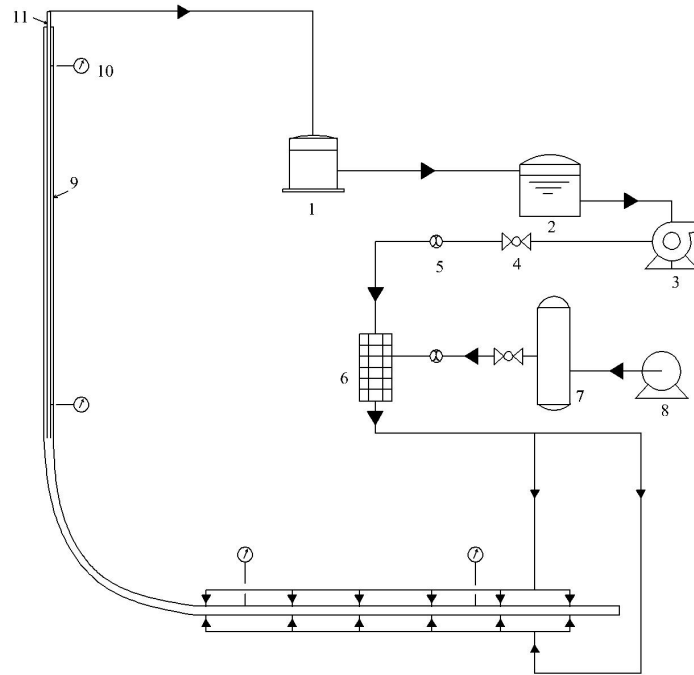
Compared with the vertical section, the energy loss of fluid flowing through the inclined section is different from that of the vertical section under the conditions of unit vertical height. When gas-liquid two-phase mixtures flow through the inclined section, it is necessary to overcome the shear stress and gravity work of the pipe wall, which is similar to the vertical section. However, due to change in trajectory in the inclined section, the flow direction of the gas-liquid flow changes when it passes through the inclined section, and the fluid will strike the pipe wall to generate additional energy loss; Compared with a vertical well with same depth, if the inclined section is longer, the friction loss that needs to be overcome is greater, resulting in greater additional energy loss. Therefore, it is more difficult to carry liquid in inclined pipe than in vertical pipe under the same pipe diameter, pressure and temperature. Generally speaking, liquid carrying in the horizontal section is the result of pressure difference. For gas-liquid two-phase under certain conditions of producing liquid and gas, liquid-carrying in horizontal section is basically possible, and the required gas velocity only needs to overcome the shear stress of gas-liquid interface and pipe wall. Through analysis and comparison, it is found that the gas velocity required for liquid-carrying in the horizontal section is lower than that of the vertical section, and it is the most difficult to carry liquid in inclined section under certain conditions.

### **2.2 Experiment**

In order to study the continuous liquid carrying and liquid loading in horizontal wells, a gas-liquid flow experiment was conducted using the wellbore of a horizontal well.

The experiment was carried out at the Laboratory of Multiphase Pipe Flow of Gas Lift Innovation Center at Yangtze University, China. The horizontal wellbore gas-liquid two-phase flow simulation experimental facility was designed and fabricated. The experimental flow chart is shown in Fig. 1. The experimental facility consists of simulation wellbore, gas-liquid steady flow regulation system, metering system and separation system. The experimental test pipe consists of a visual Perspex pipe with an inner diameter of 30 mm, a length of vertical pipe of 12.47 m, inclined pipe of 4 m, and horizontal pipe of 12.47 m. The experimental media were air and water.

During the experiment, air was supplied by the air compressor and measured by the air flow meter with a range of 0-2100 m<sup>3</sup>/h and an accuracy of  $\pm 1\%$ . Water was supplied by a liquid pump and measured by a liquid flowmeter with a range of 0-20 m<sup>3</sup>/h and an accuracy of  $\pm 0.5\%$ . After the air and water were fully mixed in a blender, the air-water mixture flowed into the test pipe. At the entrance of the test pipe, a pressure sensor with a range of 0-3.5 MPa and an accuracy of  $\pm 0.1\%$  and a temperature sensor with a range of 0-90°C and an accuracy of  $\pm 0.5\%$ , which can meet a variety of different temperature and pressure conditions, were installed. Meanwhile, the measured data was transmitted to the computer. In addition, the flow pattern transition and liquid-carrying state were visually observed and recorded using a high speed camera with a frame rate of 2000 fps and a resolution of 1920\*1080.



1-Liquid metering tank; 2-Gas-liquid separator; 3-Liquid pump; 4-Regulating valve; 5-Liquid flowmeter; 6-Blender; 7-Air storage tank; 8-Air compressor; 9-Tube; 10-Pressure sensor; 11-Casing

**Figure 1:** Flowchart of gas-liquid flow in the whole wellbore of horizontal wells

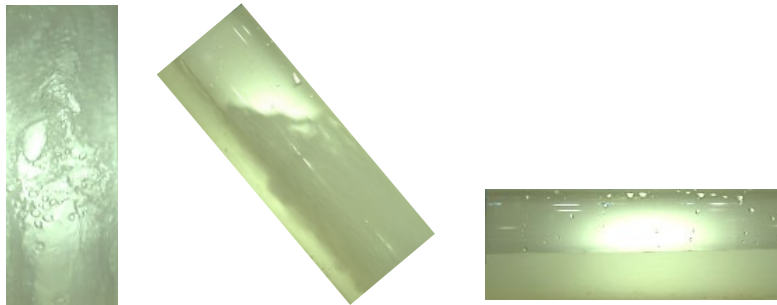
This experiment simulated the air-water flow of the whole wellbore in horizontal well within a temperature range of 28-31°C. The liquid volume flow rate was adjusted by the power of the pump and the regulating valve to 0.1 m<sup>3</sup>/h, 0.2 m<sup>3</sup>/h and 0.4 m<sup>3</sup>/h respectively. The gas volume flow rate was controlled by the regulating valve and computer with a range of 4-55 m<sup>3</sup>/h.

In this experiment, the flow pattern transition and the liquid carrying state of gas-liquid two-phase in the vertical pipe, inclined pipe and horizontal pipe were observed by adjusting the regulating valve to control injected gas volume flow rate. During the experiment, firstly, the liquid volume flow rate was adjusted to the experimental value; meanwhile, the gas volume flow rate was adjusted to the maximum value in the experiment (55 m<sup>3</sup>/h). The flow phenomena were observed and recorded when the flow process was stable; simultaneously, the data such as pressure, temperature and pressure difference were measured. After that, reduced the gas flow rate and repeated the above experimental procedure. The relevant flow parameters were tested and the flow phenomena were observed. After completing a set of experiment, changed the liquid volume and repeated the above experiment.

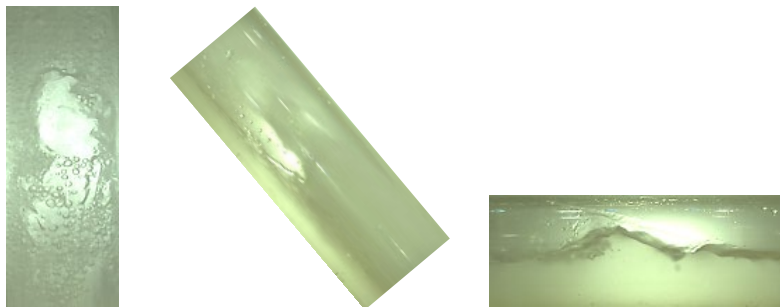
According to the experimental results, the position of the easiest to liquid loading in horizontal wells is identified from liquid-carrying conditions, flow patterns and pressure gradient in different sections during air-water flow, as follows.

*2.2.1 Liquid-carrying conditions in different sections of horizontal well*

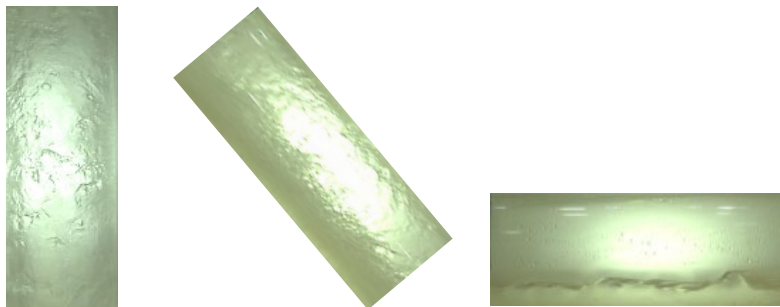
From the experimental data, the liquid carrying phenomenon of gas flow in different sections is summarized. The detailed results are shown in Fig. 2 and Tab. 1.



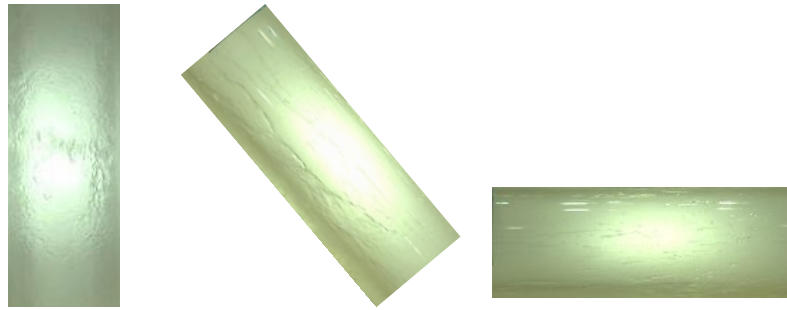
(a) 5 m<sup>3</sup>/h of gas volume



(b) 20 m<sup>3</sup>/h of gas volume



(c) 35 m<sup>3</sup>/h of gas volume

(d) 45 m<sup>3</sup>/h of gas volume**Figure 2:** Liquid-carrying phenomenon in different sections (0.2 m<sup>3</sup>/h of liquid volume)

It can be seen (Fig. 2) that the liquid phase backflows severely in vertical and inclined pipes while it starts to be carried in horizontal pipe when liquid volume is 0.2 m<sup>3</sup>/h and gas volume is 5 m<sup>3</sup>/h; the liquid backflows slightly in vertical pipe while it is partial carried in inclined pipe and carried continuously in horizontal pipe when gas volume is 20 m<sup>3</sup>/h; the liquid is carried continuously in vertical pipe while it is still partial carried in inclined pipe and carried at a high speed in horizontal pipe when gas volume is 35 m<sup>3</sup>/h; the liquid is carried at a high speed in vertical, inclined and horizontal pipe when gas volume is 45 m<sup>3</sup>/h.

**Table 1:** Liquid-carrying phenomenon in different sections (0.2 m<sup>3</sup>/h of liquid volume)

Section	Gas volume (m <sup>3</sup> /h)			
	<16	16-22	22-35	>35
Vertical	severe backflow	slight backflow	Continuous liquid-carrying	high speed liquid-carrying
Inclined	severe backflow	partial liquid-carrying		high speed liquid-carrying
Horizontal	onset of liquid-carrying	Continuous liquid-carrying	effective liquid-carrying	high speed liquid-carrying

When the gas volume is large enough, the gas well can carry liquid stably and effectively. Meantime, the flow pattern of each well section is different. The vertical section mainly presents annular flow; the inclined section presents slug flow; the horizontal section presents obvious wavy flow. When the gas well can carry liquid continuously, the liquid discharge volume at the wellhead is basically the same as the liquid production in the horizontal section. There is no liquid accumulation or huge slug reflux in the wellbore.

It can be found that it is more difficult to carry liquid in inclined section than in vertical section, and the horizontal section can basically carry liquid in horizontal wells.

*2.2.2 Flow patterns in different sections of horizontal well*

Through simulating experiment of gas-liquid flow in horizontal wells, the flow patterns in different sections are summarized, as shown in Fig. 3 and Tab. 2.

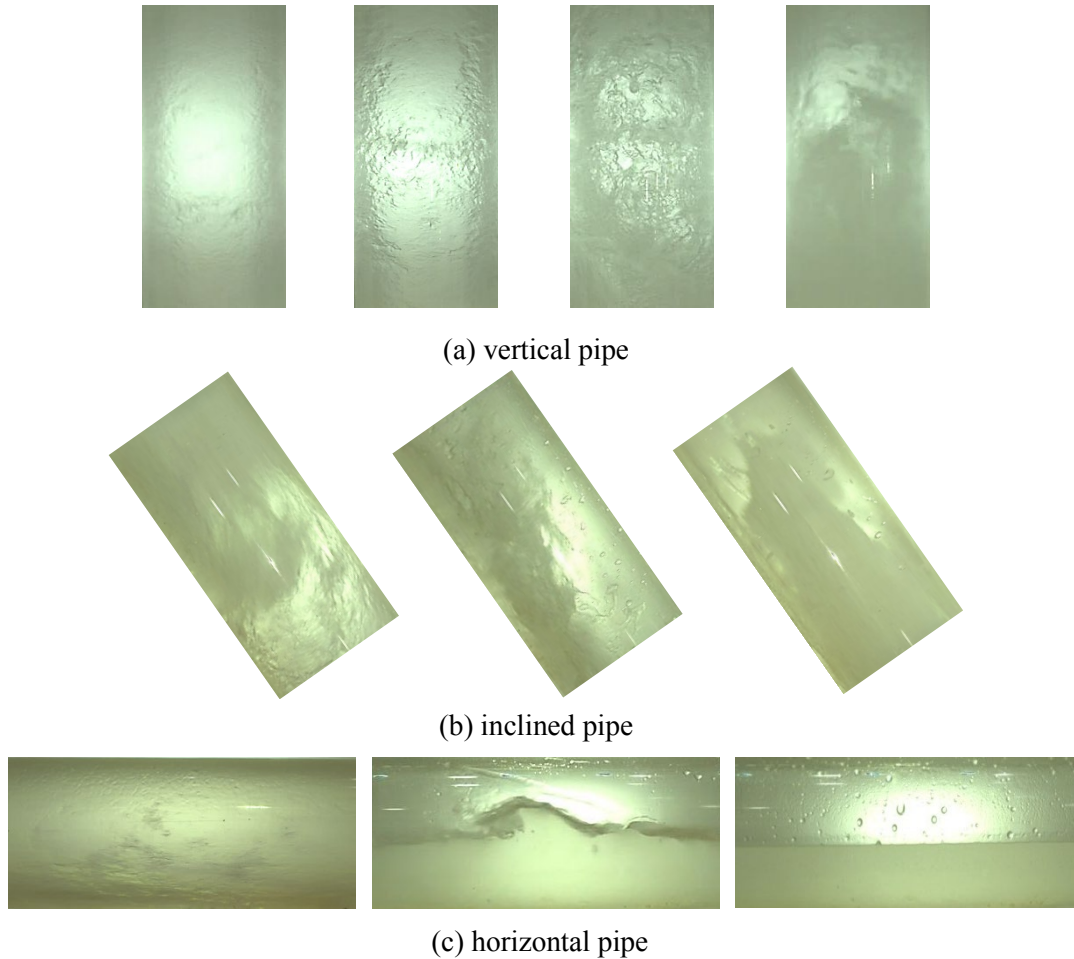


**Figure 3:** Flow pattern transition during gas flow rate decline (0.2 m<sup>3</sup>/h of liquid volume)

**Table 2:** Flow pattern transition during gas flow rate decline

section	flow pattern transition
vertical	mist flow, annular mist flow, annular flow, churn flow, slug flow
inclined	slug-annular, churn flow, slug flow
horizontal	annular flow, wavy flow, laminar flow

It can be seen (Fig. 3) that with the increase of gas flow rate, annular mist flow carrying liquid at high speed appears first in the vertical pipe under 0.2 m<sup>3</sup>/h of liquid volume; unlike the vertical pipe, slug flow always appears in the inclined pipe, and is

accompanied with backflow until flow rate high enough. When the gas flow rate is low, the liquid accumulates on the pipe wall and slides downward due to the gravity of the liquid. The falling liquid film collides with the fluid followed by the airflow, causing disturbance and forming a slug flow (gas and liquid intermittently flow, mainly a gas slug and a liquid slug alternately appearing); Provided a sufficient amount of liquid, slug flow will be formed even if the gas flow rate is not too high. The reflux of the inclined section has an effect on the flow pattern of the horizontal section. In the horizontal section, the frictional energy of the air-water interface can push the liquid from toe to root with a little pressure difference and air flow rate. The air-water two-phase flow is characterized by a relatively stratified flow, and the fluctuation of the air-water interface is not obvious. When there is liquid reflux in the inclined section, most of the liquid accumulates in the root of the horizontal section, where slug flow is easy to form. Furthermore, the liquid loading weakens the liquid carrying capacity of the horizontal section since the liquid reflux consuming part of the energy (the acceleration of liquid phase changed).

The analysis of flow pattern in horizontal wells shows that slug flow is the main flow pattern in the inclined pipe, and it is difficult to carry liquid in the whole process. When continuous liquid carrying occurs in vertical pipe and horizontal pipe, there is still a slight backflow in inclined pipe. Combining the indoor simulation experiment phenomenon and the fluid carrying process, it is found that it is the most difficult to carry liquid in the inclined section.

### 2.2.3 Pressure gradient in different sections of horizontal well

Through the simulation experiments of gas-water flow in a single pipe of horizontal well, the pressure gradient of gas-water flow in vertical pipe, inclined pipe and horizontal pipe is analyzed, as shown in Fig. 4.

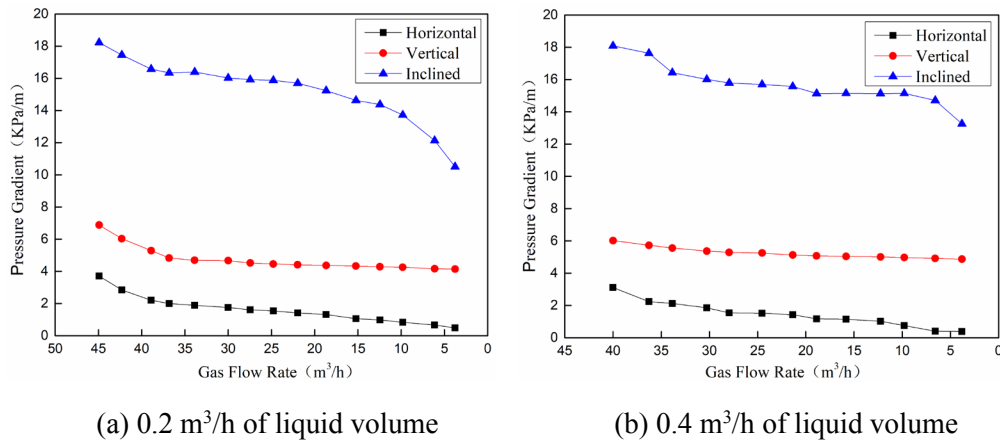


**Figure 4:** Pressure gradient of gas-water flow in horizontal well

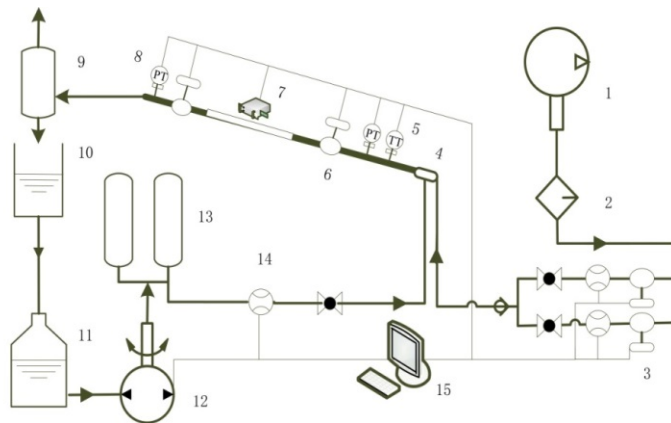
Variation of the pressure gradient with gas flow rate (Fig. 4) shows that the largest pressure gradient values are obtained in the inclined pipe during the gas-water flow, which further indicates that the inclined pipe is the most easily accumulated section of horizontal wells.

In conclusion, the horizontal and vertical pipes have little effect on the continuous liquid-carrying of the horizontal gas wells, and the liquid loading in the inclined pipe is the main factor to cause liquid loading in the horizontal gas wells. Therefore, it is necessary to focus on the analysis of liquid carrying in the inclined pipe when studying the problem of continuous liquid carrying in horizontal gas wells.

### 3 Critical liquid carrying experiment in the inclined pipe

#### 3.1 Experimental facility

108 tests for gas-liquid flow and liquid carrying were conducted in the inclined pipe to determine the position of the most prone to liquid loading in the inclined pipe and the critical gas flow rate at different angles. The experiment is conducted at the Laboratory of Multiphase Pipe Flow of Gas Lift Innovation Center, CNPC. The experimental test pipe consists of a 7 m perspex pipe with an inner diameter of 60 mm. The experimental flow chart is shown in Fig. 5.



1-Air compressor; 2-Air dryer; 3-Aerovale; 4-Blender; 5-Temperature sensor; 6-Fast valve; 7-High speed camera; 8-Pressure sensor; 9-Gas-liquid separator; 10-Metering tank; 11-Water tank; 12-Liquid pump; 13-Buffer tank; 14-Flowmeter; 15-Computer

**Figure 5:** Flowchart of gas-liquid flow liquid-carrying experiment

In the experiment, the pressure of the test pipe was set to 0.2 MPa and 0.5 MPa and the inclined angles were  $6^\circ$ ,  $10^\circ$ ,  $15^\circ$ ,  $30^\circ$ ,  $45^\circ$ ,  $60^\circ$  and  $74^\circ$  from the horizontal. The liquid volume flow rate was  $0.1 \text{ m}^3/\text{h}$ ,  $0.2 \text{ m}^3/\text{h}$ , and  $0.4 \text{ m}^3/\text{h}$  while the gas flow rate was controlled with a range of  $100\text{-}700 \text{ m}^3/\text{h}$  (standard condition). The experimental media were air and water.

Under the selected pressure conditions of 0.2 MPa or 0.5 MPa, the injected liquid flow rate was kept constant. By changing the injected gas volume, the state of liquid phase in the experimental pipe under different inclined angles was observed. When a stable critical liquid-carrying state in the experimental pipe section was reached, the experimental data including the injected gas flow rate, the injected water flow rate, pressure, pressure difference, and temperature were recorded by computer. Meanwhile,

the flow patterns were recorded by a high speed camera. After completing a set of experiments, the pressure was changed and the above experiment was repeated to obtain critical liquid-carrying gas flow rate under different pressure.

During the experiment, the criterion of airflow reaching a stable critical liquid-carrying state under various working conditions was the same liquid volume at the outlet and the inlet. According to the experimental test data, the graph of the liquid holdup changing with gas flow rate under certain inclined angle and different liquid flow rate is plotted, and the critical liquid-carrying gas flow rate determined by the experiment is marked, as shown in Fig. 6.

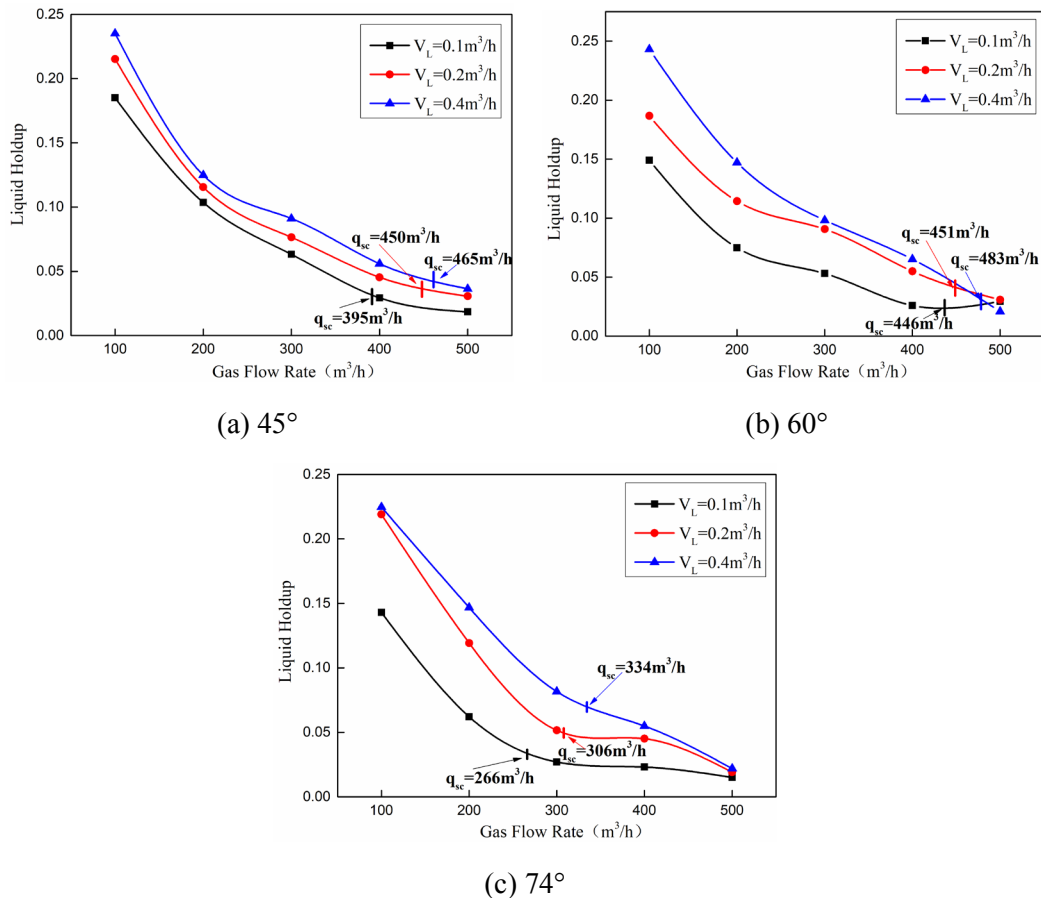


**Figure 6:** Liquid holdup curves at 0.2 MPa

It is found that the liquid holdup in wellbore increases as the gas flow rate decreases. By comparing the change of liquid holdup before and after the critical gas flow rate, it can be found that when the gas flow rate is greater than the critical liquid-carrying flow rate, the liquid holdup changes more gently with the gas flow rate; while the gas flow rate is less than the critical liquid-carrying flow rate, the liquid holdup increases obviously with the

decrease of the gas flow rate. This proves that the criterion for determining the critical liquid-carrying gas flow in the experiment is correct.

It can be inferred from Fig. 6 that the liquid holdup increases first and then decreases with the inclined angle increasing. This can be attributed to the redistribution on the fluid. When the inclined angle changes, the gravity and viscous resistance have a huge impact on the liquid phase, and ultimately lead to the change of slip velocity and liquid holdup. Under a certain amount of gas and liquid volume, the gravity on the liquid reduces the liquid velocity with the inclined angle increasing, which corresponds to an increase in the slippage and liquid holdup. With a further increase of inclination, the liquid is overlapped in the pipe, which will reduce the slippage between the gas and liquid, thus the liquid holdup decreases. When the inclined angle is about 50°, the liquid holdup reaches the maximum.

### 3.2 Liquid loading in the inclined pipe

The critical gas flow rate measured under different pressure and inclined angles in the experiment were plotted as shown in Fig. 7. It can be found that with the angle increasing, the critical gas velocity increases first and then decreases. The critical gas velocity reaches its maximum when the inclined angle at the range of 45-60°.

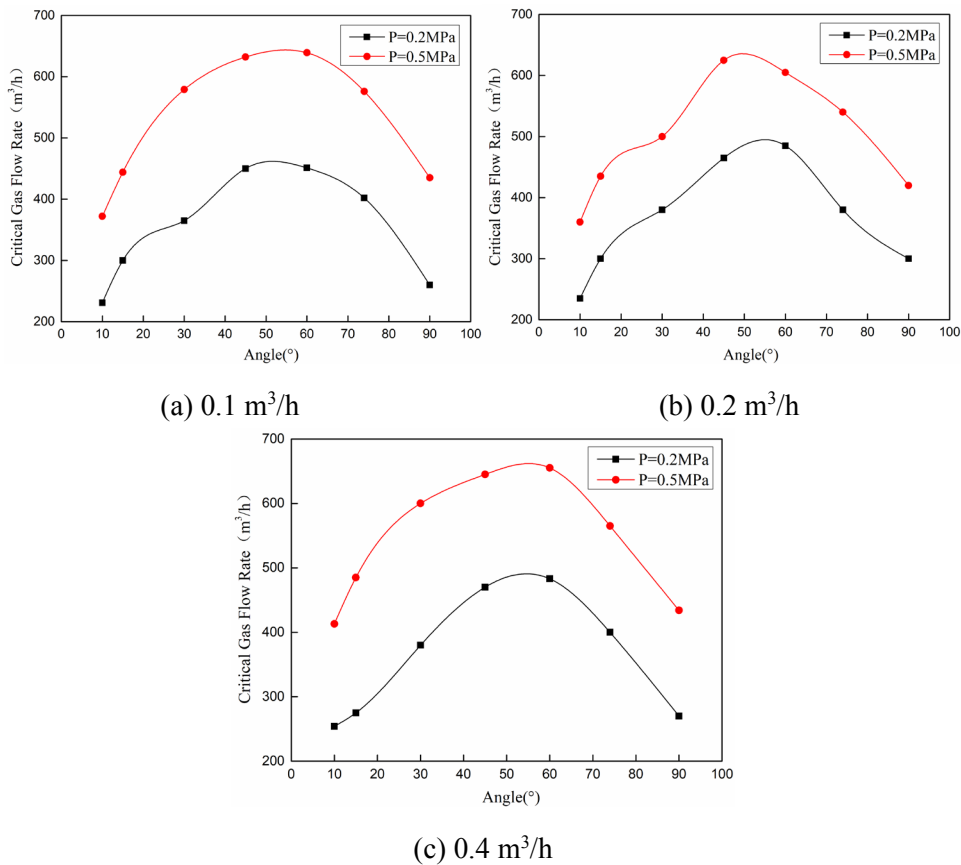
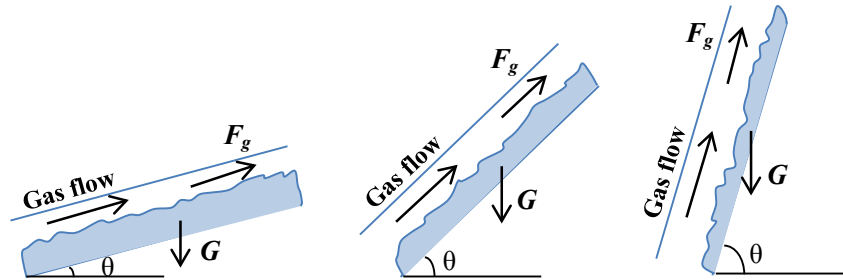


Figure 7: Critical liquid-carrying gas flow rate curves

This is because of the force balance on the film attached to bottom of the inclined pipe. To take the liquid film as the force analysis object, as shown in Fig. 8. When the force is balanced, the gas drag force to the liquid film is equal to the component of the gravity along the gas flow direction. Meanwhile, there is no friction between the film and the pipe.



**Figure 8:** Schematic of the force balance on the liquid film at the bottom of an inclined pipe

The force balance per unit length on the film along the gas flow direction can be given as

$$F_g = G \sin \theta \quad (1)$$

where  $F_g$  is the gas drag force,  $G$  is the gravity per height of the bottom film, and  $\theta$  is the angle from the horizontal.

With the inclined angle increasing, the circumferential distribution of the liquid film becomes more uniform and the liquid film thickness decreases, which leads to the gravity of the liquid film is decreased. Namely, a larger inclination means a larger  $\sin \theta$  and a smaller  $G$  in Eq. (1). At low inclination, the rate of increase in  $\sin \theta$  is larger than the rate of decrease in  $G$  when the inclination increases, which results in a larger  $F_g$  to drag the film for prevention reflux. However, a further increase will lead to an opposite change of  $F_g$  when the inclination reaches a certain point, which corresponds to a decrease in gas velocity.

It can be seen from Fig. 7 that the critical gas flow rate increases with the pressure of gas well increasing. When the pressure is increasing, partial kinetic energy transforms into internal energy due to gas molecules squeezing. At the same time, the friction between the gas molecules and the pipe wall increases and the energy loss is significant, which ultimately causes the decrease of gas flow rate and drag force of the gas carrying liquid in the wellbore.

#### 4 Optimization of prediction model

Through the dynamic simulation of gas-liquid two-phase flow and critical liquid-carrying flow under different inclined angles, pressure and flow rate in inclined pipe, the experimental results are compared with the calculation results of several commonly used prediction models. The results are shown in Fig. 9.

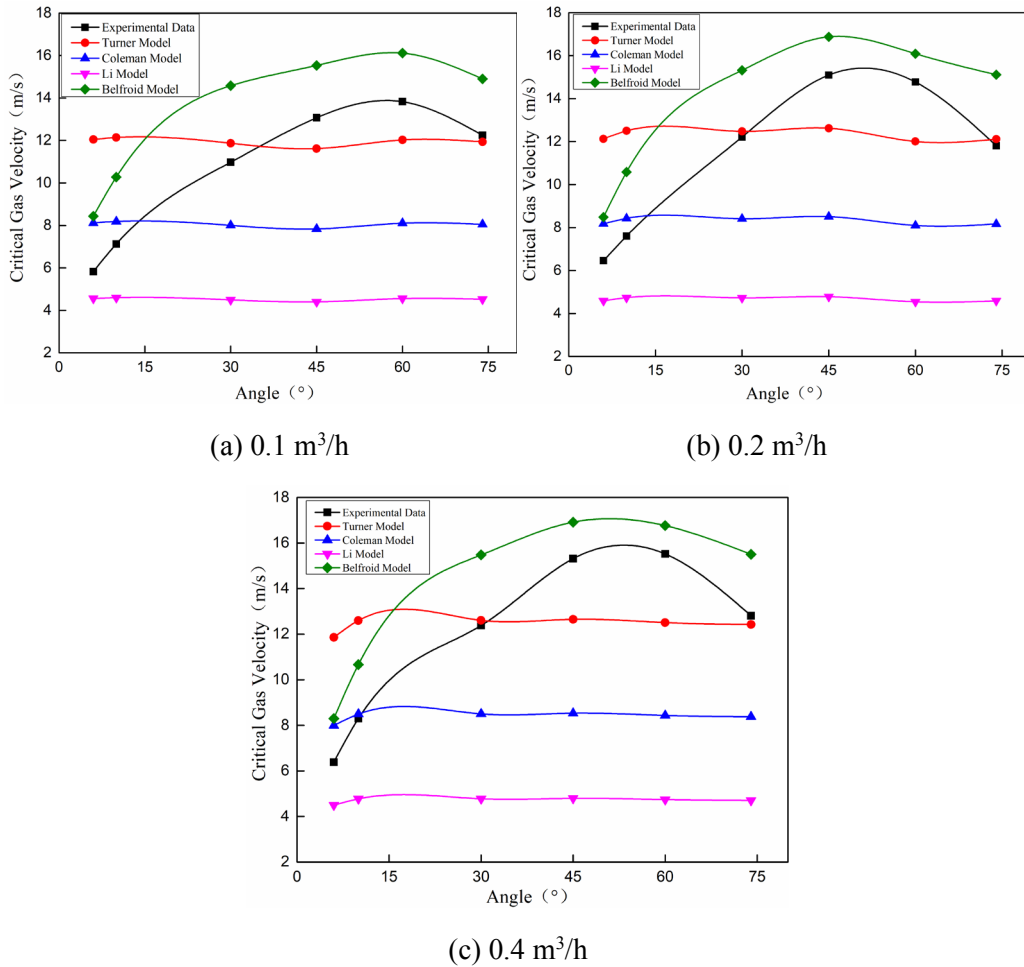


**Figure 9:** Comparison of experimental results with calculated values of the models

It can be seen that the errors of the Turner et al. (1969) model, Coleman et al. (1991) model and Li et al. (2002) model are large, mainly because these models are derived based on the droplet theory. But the theory and experiment have proved that liquid phase exists and is carried mainly in the form of liquid film. Furthermore, these models are based on the condition of vertical pipe, while the force state of liquid phase in inclined pipe is quite different from that in vertical pipe. The Belfroid et al. (2008) model over-predicts the experimental data. This is because the model is based on the derivation of directional well. The model considers that the droplets move upward along the central line of the wellbore, which is inconsistent with the actual liquid carrying situation. Only the trend of Belfroid et al. (2008) model is more in line with the experimental results, although the numerical values still have a great deviation.

Using the experimental results, the Belfroid et al. (2008) model (Eq. (2)) is optimized and fitted with the experimental data. A modified model (Eq. (3)) for predicting critical gas velocity in inclined pipe is obtained.

$$v_{cr} = 6.6 \left[ \frac{(\rho_l - \rho_g) \sigma}{\rho_g^2} \right]^{0.25} \frac{[\sin(1.7\theta)]^{0.38}}{0.74} \quad (2)$$

$$v_{cr} = 6.6 \left[ \frac{(\rho_l - \rho_g) \sigma}{\rho_g^2} \right]^{0.25} \frac{[\sin(1.7\theta)]^{0.46}}{0.85} \quad (3)$$

where  $v_{cr}$  is the critical gas velocity,  $\rho_l$  is the density of liquid,  $\rho_g$  is the density of gas,  $\sigma$  is the surface tension, and  $\theta$  is the inclined angle.

The formula of critical gas flow rate can be written as:

$$q_{sc} = 2.5 \times 10^8 \frac{Apv_{cr}}{ZT} \quad (4)$$

where  $q_{sc}$  is the critical gas flow rate,  $A$  is the tube area,  $p$  is the pressure,  $T$  is the temperature, and  $Z$  is the compression factor.

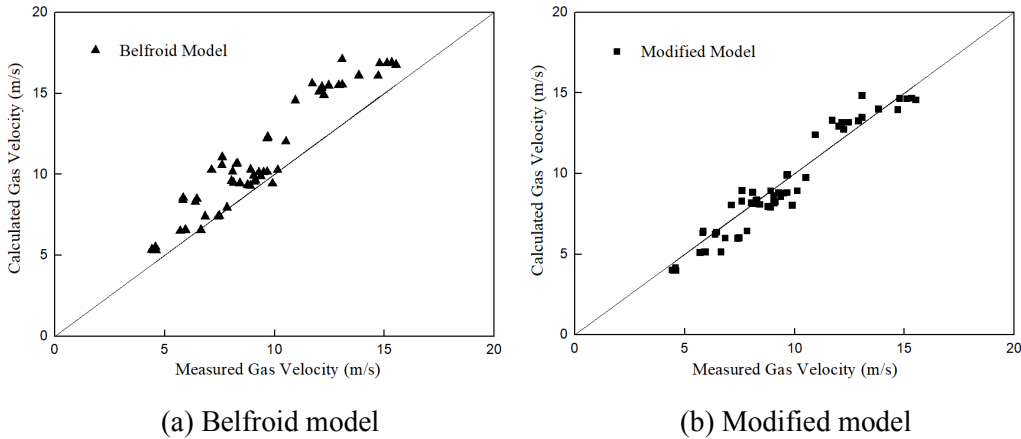


**Figure 10:** Comparison of calculated gas velocity by models and test data

A total of 56 experimental data can be used to evaluate the models. The comparison of the predicted and measured critical gas velocity is shown in Fig. 10. Error statistics are defined as follows:

Error of critical gas velocity:

$$e_{ri} = (\text{predicted} - \text{measured}) / \text{measured} \quad (5)$$

Average percent error of critical gas velocity:

$$E_1 = \frac{1}{n} \sum e_{ri} \quad (6)$$

Average absolute percentage error of critical gas velocity:

$$E_2 = \frac{1}{n} \sum |e_{ri}| \quad (7)$$

Standard deviation of critical gas velocity:

$$E_3 = \sqrt{\frac{\sum (e_{ri} - E_1)^2}{n - 1}} \tag{8}$$

**Table 3:** Error statistics of critical gas velocity

Model	E <sub>1</sub> /%	E <sub>2</sub> /%	E <sub>3</sub> /%
Belfroid model	17.83	18.08	23.92
Modified model	2.85	8.3	9.76

Comparison with the modified model, the Belfroid et al. (2008) model overestimates the critical gas velocity. The average absolute errors of the predicted by the modified model and the Belfroid et al. (2008) model from the measured critical velocity are 8.39% and 18.08%, respectively. Therefore, the modified model has better performance and smaller deviation for prediction of liquid loading than the Belfroid model.

### 5 Field data validation

In order to verify the reliability of the new model, the field data of 25 horizontal gas wells are used to validate the new model and the widely used prediction models. Among these wells, there are 6 gas wells suffering from liquid loading and 19 gas wells with unloading. In Eq. (3), it is obvious that when the inclined angle is 53°, the critical gas velocity reaches the maximum. Therefore, 53° is selected as the most difficult to liquid-carrying point to calculate the critical gas flow rate.

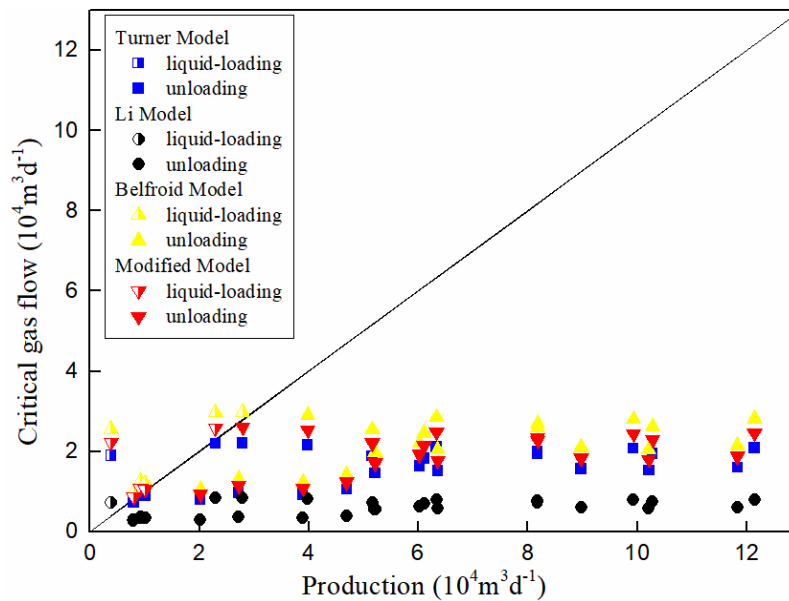


**Figure 11:** Comparison of calculated gas flow rate by models and field data

**Table 4:** Results of model prediction

Model	Liquid-loading gas wells		Unloading gas wells		Total	
	wells	accuracy	wells	accuracy	wells	accuracy
Turner	1/6	16.67%	19/19	100%	20/25	80%
Li	1/6	16.67%	19/19	100%	20/25	80%
Belfroid	5/6	83.33%	18/19	94.74%	23/25	92%
New	5/6	83.33%	19/19	100%	24/25	96%

Fig. 11 presents the comparison of the calculated gas flow rate by the three models and the field data. The diagonal line represents that whether a gas well is suffering from liquid loading. If a data point of a liquid-loading gas well in the figure is above the diagonal line, a data point of an unloading gas well is under the diagonal line, namely, the result of model prediction is correct. Otherwise, the result of model prediction is wrong. It can be seen from Fig. 11 that the Li model is too conservative in prediction of liquid loading. The values of calculated gas flow rate of Turner model are larger than that of Li model, but the two models misjudge 5 gas wells suffering from liquid loading, similarly. The Belfroid model misjudges 1 gas well suffering from liquid loading and 1 gas well with unloading. The new model has more accurate prediction in loading and unloading gas wells with 1 misjudgment of liquid loading gas well (see Tab. 4). From the validation against the field data, it can be concluded that the new model can provide an accurate approach to predicting liquid loading of a horizontal gas well.

## 6 Conclusion

The gas-liquid two phase flow experiment in the whole wellbore of a horizontal well and critical liquid carrying experiment in inclined pipe section were conducted on the multiphase flow experimental platform. A modified Belfroid et al. (2008) model is proposed to predict critical gas flow rate in horizontal gas wells. The following conclusions can be drawn from the study:

- (1) By observing the experimental phenomenon of gas-water flow in a horizontal well and comparing the pressure gradient of each section, it is shown that the inclined section is the position of the most easily to liquid loading in horizontal gas wells.
- (2) With the increase of inclined angle, the critical gas velocity increases first and then decreases, and angle of the most easily to liquid loading ranges from 45° to 60°.
- (3) The trend of the critical gas velocity calculated by the Belfroid et al. (2008) model is consistent with the experimental results, but the calculated value is larger than the experimental value. A modified model for predicting critical gas velocity of inclined section in horizontal gas wells is proposed by fitting with experimental data and correcting the angle term of the Belfroid et al. (2008) formula.
- (4) The modified model is validated with field data. It shows that the new model is more accurately for prediction of liquid loading compared with other models, verifying the reliability of the new model.

**Acknowledgement:** The authors like to express appreciation to the support given by the major national science and technology special project: Research and Application of Key Technologies for Oil Production and Gas Recovery in Complex Carbonate Reservoirs in Central Asia and Middle East (2017ZX05030-005) and Scientific Research Startup Fund Project for Introducing Talent of Kunming University of Science and Technology (KKSJ20180502).

## References

**Alsaadi, Y.; Pereyra, E.; Torres, C.** (2015): Liquid loading of highly deviated gas wells from 60° to 88°. *SPE Annual Technical Conference and Exhibition*, pp. 28-30.

**Barnea, D.** (1986): Transition from annular flow and from dispersed bubble flow-unified models for the whole range of pipe inclinations. *International Journal of Multiphase Flow*, vol. 12, no. 5, pp. 733-744.

**Belfroid, S. F. C.; Schiferli, W.; Alberts, G. J. N.; Veeken, C. A. M.; Biezen, E.** (2008): Predicting onset and dynamic behaviour of liquid loading gas wells. *SPE Annual Technical Conference and Exhibition*, pp. 21-24.

**Chen, D. C.; Yao, Y.; Han, H.; Fu, G.; Song, T. J. et al.** (2016): A new prediction model for critical liquid-carrying flow rate of directional gas wells. *Natural Gas Industry*, vol. 36, no. 6, pp. 40-44.

**Coleman, S. B.; Clay, H. B.; McCurdy, D. G.; Norrls, H. L.** (1991): A new look at predicting gas-well load-up. *Journal of Petroleum Technology*, vol. 43, no. 3, pp. 329-333.

**Guo, B. Y.; Ghalambor, A.; Xu, C. C.** (2006): A systematic approach to predicting liquid loading in gas wells. *SPE Production & Operations*, vol. 21, no. 1, pp. 81-88.

**Jiang, J.; Zou, Y. F.; Zhou, X. F.; Fu, C. M.; Liu, Y. H.** (2012): Prediction of critical liquids carrying flow rate for horizontal wells and its application. *Natural Gas and Oil*, vol. 30, no. 3, pp. 45-48.

**Li, L.; Zhang, L.; Yang, B.; Yin, Y.; Li, D. W.** (2012): Prediction method of critical liquid-carrying flow rate for directional gas wells. *Oil & Gas Geology*, vol. 33, no. 4, pp. 650-654.

**Li, M.; Li, S. L.; Sun, L. T.** (2001): New view on continuous-removal liquids from gas wells. *SPE Production & Facilities*, vol. 17, no. 1, pp. 42-46.

**Li, Y. S.; Li, X. F.; Teng, S. N.; Liu, X. D.; Xu, D. R. et al.** (2014): Research of gas well liquid-carrying critical rate model. *Journal of Engineering Thermophysics*, vol. 35, no. 2, pp. 291-294.

**Liu, Y. H.; Luo, C. C.; Zhang, L. H.; Liu, Z. B.; Xie, C. Y. et al.** (2018): Experimental and modeling studies on the prediction of liquid loading onset in gas wells. *Journal of Natural Gas Science and Engineering*, vol. 57, pp. 349-358.

**Luo, S.; Kelkar, M.; Pereyra, E.; Sarica, C.** (2014): A new comprehensive model for predicting liquid loading in gas wells. *SPE Production & Operations*, vol. 29, no. 4, pp. 337-349.

**Nosseir, M. A.; Darwich, T. A.; Sayyoub, M. H.; EI Sallaly, M.** (2000): A new approach for accurate prediction of loading in gas wells under different flowing conditions. *SPE Production & Facilities*, vol. 15, no. 4, pp. 241-246.

**Shekhar, S.; Kelkar, M.; Hearn, W. J.; Hain, L. L.** (2017): Improved prediction of liquid loading in gas wells. *SPE Production & Operations*, vol. 32, no. 4, pp. 539-550.

**Shi, J. T.; Sun, Z.; Li, X. F.** (2016): Analytical models for loading in multifractured horizontal gas wells. *SPE Journal*, vol. 21, no. 2, pp. 471-487.

**Turner, R. G.; Hubbard, M. G.; Dukler, A. E.** (1969): Analysis and prediction of minimum flow rate for the continuous removal of liquid from gas wells. *Journal of Petroleum Technology*, vol. 21, no. 11, pp. 1475-1482.

**van 't Westende, J. M. C.; Kemp, H. K.; Belt, R. J.; Portela, L. M.; Mudde, R. et al.** (2007): On the role of droplets in co-current annular and churn-annular pipe flow. *International Journal of Multiphase Flow*, vol. 33, no. 6, pp. 595-615.

**Veeken, K.; Hu, B.; Schiferli, W.** (2010): Gas-well liquid-loading-field-data analysis and multiphase-flow modeling. *SPE Production & Operations*, vol. 25, no. 3, pp. 275-284.

**Wang, Q.; Li, Y. C.; Wang, Z. B.; Cheng, J. J.** (2014): Experimental study and model evaluation on continuous liquid removal in horizontal gas well. *Journal of Southwest Petroleum University (Science & Technology Edition)*, vol. 36, no. 3, pp. 139-145.

**Wang, Y. Z.; Liu, Q. W.** (2007): The mechanism of continuously removing liquids from gas wells. *Petroleum Geology & Oil-Field Development in Daqing*, vol. 26, no. 6, pp. 82-85.

**Wang, Z. B.; Guo, L. J.; Zhu, S. Y.; Nydal, O. J.** (2018): Prediction of the critical gas velocity of liquid unloading in a horizontal gas well. *SPE Journal*, vol. 23, no. 2, pp. 1-16.

**Wang, Z. B.; Li, Y. C.** (2012): The mechanism of continuously removing liquids from gas wells. *Acta Petrolei Sinica*, vol. 33, no. 4, pp. 681-686.

**Wang, Z.; Bai, H.; Zhu, S.; Zhong, H.; Li, Y.** (2015): An entrained-droplet model for prediction of minimum flow rate for the continuous removal of liquids from gas wells. *Society of Petroleum Engineers*, vol. 20, no. 5.

**Xiao, G. M.; Li, Y. C.; Yu, X.** (2010): Theory and experiment research on the liquid continuous removal of horizontal gas well. *Journal of Southwest Petroleum University (Science & Technology Edition)*, vol. 32, no. 3, pp. 122-126.

**Yang, W. M.; Wang, M.; Chen, L.; Wu, J. C.; Yu, P. X.** (2009): A prediction model on calculation of continuous liquid carrying critical production of directional gas wells. *Natural Gas Industry*, vol. 29, no. 5, pp. 82-84.

**Zhang, L. H.; Luo, C. C.; Liu, Y. H.; Zhao, Y. L.; Xie, C. Y. et al.** (2019): Research progress in liquid loading prediction of gas wells. *Natural Gas Industry*, vol. 39, no. 1, pp. 57-63.

**Zhou, D.; Yuan, H.** (2010): A new model for predicting gas-well liquid loading. *Society of Petroleum Engineers*, vol. 25, no. 2.